Characterization and reactivity of molybdenum oxide catalysts supported on anatase and rutile polymorphs of titania

ARTICLE *in* APPLIED CATALYSIS A GENERAL · FEBRUARY 2001

Impact Factor: 3.94 · DOI: 10.1016/S0926-860X(00)00724-9

ELSEVIER

Applied Catalysis A: General 208 (2001) 291–305

APPLIED CATALYSIS A: GENERAL

www.elsevier.com/locate/apcata

Characterization and reactivity of molybdenum oxide catalysts supported on anatase and rutile polymorphs of titania

Komandur V.R. Chary*, Thallada Bhaskar, Kothapalli Kalyana Seela, Katar Sri Lakshmi, Kondakindi Rajender Reddy

Catalysis Section, Indian Institute of Chemical Technology, Hyderabad 500007, India

Received 1 May 2000; received in revised form 24 June 2000; accepted 3 July 2000

Abstract

A series of MoO_3 catalysts with Mo loadings, ranging from 2–12% w/w, supported on TiO_2 (anatase) and TiO_2 (rutile) were investigated by X-ray diffraction, temperature programmed reduction (TPR), ^1H magic angle spinning (MAS) NMR and oxygen chemisorption measurements. Dispersion of molybdena was determined by the oxygen chemisorption at 623 K and by a static method on the samples prereduced at the same temperature. At low Mo loadings, i.e. below 6% Mo, molybdenum oxide was found to be present in a highly dispersed state. Oxygen chemisorption results suggest that MoO_3 particles disperse better on TiO_2 (anatase) than when they are supported on TiO_2 (rutile). ^1H magic-angle-spinning NMR spectra of MoO_3 catalysts supported on anatase and rutile polymorphs reveal the presence of two types of OH groups on the surface: OH groups of acidic nature and the basic OH groups. Temperature programmed reduction profiles of MoO_3/TiO_2 samples suggest that the reduction of MoO_3 to Mo proceeds in two stages and the reducibility of MoO_3 increases with Mo loading in the catalysts. The catalytic properties were evaluated for the vapor-phase ammoxidation of 3-picoline to nicontinonitrile and are related to oxygen chemisorption sites on the surface.

Keywords: Molybdena; Titania; Chemisorption; NMR; Ammoxidation

1. Introduction

Supported molybdenum oxide catalysts have been extensively investigated in the recent past because of their importance in many industrially important reactions, including hydrodesulfurization (HDS), partial oxidation and metathesis of olefins [1–10]. In many reactions catalyzed by molybdenum oxide, however, the active component is often employed on supported oxide viz., Al_2O_3, TiO_2, SiO_2 or mixed with oxides such as vanadium. The efficiency of supported molybdenum oxide catalysts mainly depends on the dispersion of active phase, which in turn can be greatly influenced by the nature of supported oxide and the method of preparation of the catalysts. Many studies have been performed during the last two decades, relating the structural information of supported molybdenum oxides/sulfides with their catalytic properties [11–24].

Among the supported molybdena systems, MoO_3/TiO_2 catalysts have been the subject of many recent investigations [4–24,36]. Kim et al. [24–27] have extensively studied the interaction of molybdena with the two crystallographic modifications of titania, i.e. anatase and rutile, and also with other oxide supports. They investigated the physico-chemical properties of

* Corresponding author. Tel.: +91-40-7171510; fax: +91-40-7173387.
E-mail address: kvrchary@iict.ap.nic.in (K.V.R. Chary).

0926-860X/01/$ – see front matter
PII: S0926-860X(00)00724-9

MoO_3/TiO_2 catalysts prepared by equilibrium adsorption method to elucidate the adsorption phenomena in the impregnating solution [24]. Furthermore, they determined the influence of the structure and the corresponding surface properties of adsorbed monolayer species on the catalytic activity of methanol oxidation. TiO_2 as a support has received great attention in catalysis research over the last two decades because of the interaction between group VIII metals and certain reducible oxides [28]. In recent years the development of high-resolution solid state NMR spectroscopy provided new possibilities for studying the adsorption and catalysis. The use of magic angle spinning (MAS) of the samples for narrowing of NMR lines makes it possible to obtain high-resolution NMR spectra of solid catalysts and adsorbed molecules. In ^{1}H MAS NMR spectra of various acidic and basic catalysts, signals from different surface OH groups bound to certain elements are often resolved, and such results allow an accurate measurement of their chemical shifts. Recently, Mastikhin et al. [29] reviewed the application of ^{1}H NMR studies of a variety of heterogeneous catalysts. Enriquez et al. [30] reported the effect of distribution of OH groups on the localization of surface water on anatase. Chary et al. [31] reported characterization of molybdenum oxide catalysts supported on titania by ^{1}H MAS NMR spectroscopy. Mastikhin and Nosov [32] reported ^{1}H NMR studies of pure titania samples. In the present investigation, we report characterization of MoO_3 supported on TiO_2 (anatase) and TiO_2 (rutile) by X-ray diffraction (XRD), temperature programmed reduction (TPR), ^{1}H MAS NMR and oxygen chemisorption methods. The catalytic properties were evaluated during vapor phase ammoxidation of 3-picoline. The purpose of this work is to estimate the dispersion of molybdena supported on TiO_2 (anatase) and TiO_2 (rutile) and also to identify the changes in the structure of the molybdenum oxide phase as a function of the active component loading with respect to crystallographic modification of TiO_2 support. Furthermore, the catalytic properties have been correlated with the oxygen chemisorption sites.

2. Experimental

A series of MoO_3 catalysts with Mo loadings ranging from 2−12% w/w supported on anatase TiO_2 (Ti-Oxide UK Ltd., SA 92 $m^2\,g^{-1}$) and rutile TiO_2 (Ti-Oxide UK Ltd., SA 33 $m^2\,g^{-1}$) were prepared by incipient wetting of the support using aqueous ammonium heptamolybdate solution at pH 8. The catalysts were dried at 383 K for 16 h and subsequently calcined at 773 K for 6 h.

Oxygen chemisorption was measured by a static method using an all-Pyrex glass system capable of attaining a vacuum of 10^{-6} Torr. The details of this experimental set-up are given elsewhere [33]. Prior to oxygen chemisorption measurements, the catalysts were reduced in a flow of hydrogen (40 ml min^{-1}) at 623 K for 2 h and evacuated at the same temperature for 1 h. The oxygen chemisorption uptakes were determined as the difference of two successive adsorption isotherms measured at 623 K. The surface areas of the catalysts were determined by the BET method using nitrogen physisorption at 77 K. XRD studies of the calcined catalysts were recorded on a Philips diffractometer using Ni filtered Cu Kα radiation.

^{1}H MAS NMR spectra were obtained on a Bruker CXP-300 spectrometer at 300.066 MHz, using 50 kHz. The $\pi/2$ radiation in pulse was 5 ms and the pulse repetition frequency was 0.2 Hz. Prior to NMR experiments, the samples were placed in special NMR tubes of 7 mm o.d. and 12 mm length and then evacuated at 523 K at 10^{-3} Pa for 24 h. The spinning of the samples was performed in quartz rotors at a frequency of 3–3.5 kHz using a probe with minimal background signal. The probe head, rotor, and the sample tubes were dried to remove any traces of water from their outside surfaces. Chemical shifts were measured relative to tetramethylsilane (TMS) as an external reference.

TPR studies were conducted on an Autochem 2910 (Micromeritics, USA) instrument. The unit has a programmable furnace with a maximum operating temperature of 1373 K. The instrument was connected to a computer which performs tasks such as programmed heating and cooling cycles, continuous data recording, gas valve switching, data storage and analysis.

In a typical experiment for TPR, about 250 mg of oven-dried sample (dried at 373 K for 16 h) was taken in a U-shaped quartz sample tube. The catalyst was packed between two plugs of quartz wool in one side of the quartz tube. The temperature was monitored with the aid of thermocouples located near the sample from outside and also on the top of the sample. Highly

sensitive mass-flow controllers (Brooks, USA) were used for monitoring the gas flows. Prior to TPR studies, the catalyst sample was pretreated by passing helium purified by molecular sieves (50 ml/min) at 673 K for 2 h. After pretreatment the sample was cooled to ambient temperature. The reducing gas consists of 5% hydrogen and the balance argon, which is purified by passing (50 ml/min) through oxy-trap and 4 Å molecular sieves. The water vapor produced during reduction of the catalyst was condensed with a cold trap which consists of isopropanol saturated with liquid nitrogen. The hydrogen concentration in the effluent stream was monitored with the thermal conductivity detector and the areas under the peaks were integrated using GRAMS/32 software. T_{max} calibration of the TCD was performed by reduction of a known amount of high purity Ag_2O to silver, a method which was found to be more reliable and reproducible than sending known volumes of hydrogen pulses through the reactor.

A down flow fixed bed reactor operating at atmospheric pressure and made of Pyrex glass was used to test the catalysts during ammoxidation of 3-picoline to nicotinonitrile. About 2 g of the catalyst diluted with an equal amount of quartz grains were charged into the reactor and were supported on a glass wool bed. Prior to introducing the reactant 3-picoline with a syringe pump, the catalyst was reduced at 723 K for 2 h in purified hydrogen flow (40 ml/min). After the prereduction, the reactor was fed with 3-picoline, ammonia and air, keeping the mole ratio of 3-picoline:H_2O:NH_3:Air at 1:13:11:44. The reaction was carried out at various temperatures ranging from 573 to 723 K. The liquid products, mainly nicotinonitrile, were analyzed by a Hewlett-Packard 6890 gas chromatograph equipped with a flame ionization detector using OV-17 column. Traces of carbon oxides were also formed during the reaction.

3. Results and discussion

Powder XRD patterns of MoO_3 catalysts supported on TiO_2 (anatase) and TiO_2 (rutile) are shown in Figs. 1 and 2, respectively. At low Mo loadings, the diffractograms did not indicate the presence of characteristic peaks due to MoO_3 (Fig. 1). XRD lines at $d = 3.81$, 3.26 and 2.36 Å appeared only at higher Mo loadings due to crystalline MoO_3 phase. The most intense XRD line due to MoO_3, corresponding to the (021) plane at $d = 3.26$ Å, was observed only beyond 6% w/w of Mo and also in higher Mo loadings on anatase and rutile supports (Fig. 1c–f and 2c–f). The intensity of this peak increases with increase of Mo loading in the catalyst. The XRD patterns also indicate that no characteristic peaks were found due to formation of a mixed oxide phase of MoO_3 and TiO_2 even at the highest Mo loading in the catalyst. The absence of XRD peaks due to MoO_3 at lower compositions of the catalysts indicates that the MoO_3 phase is present in a highly dispersed or amorphous state on the surface of TiO_2. However, the possibility cannot be ruled out for the presence of MoO_3 crystallites having size less than 40 Å at low Mo loadings in the catalysts, which is beyond the detection capacity of the powder XRD technique. XRD patterns of MoO_3/TiO_2 (rutile) are shown in Fig. 2. As observed in the case of Mo/TiO_2 (anatase) samples, in rutile supported catalysts also the XRD peaks due to MoO_3 were absent at low Mo loadings. However, crystalline MoO_3 appeared from 6% 'Mo' loading onwards ($d = 3.81$ Å) along with very intense peaks due to TiO_2 (rutile).

Oxygen chemisorption measurements were performed by a static method to determine the dispersion of molybdenum oxide on titania. As described by Oyama et al. [14], the prereduction of sample and subsequent oxygen chemisorption were carried out at 623 K. Fig. 3 shows the oxygen uptake at 623 K for various MoO_3/TiO_2 (anatase) and MoO_3/TiO_2 (rutile) catalysts plotted as a function of Mo loading. The amount of oxygen chemisorbed was calculated using the double isotherm method described elsewhere [34]. Pure TiO_2 supports did not chemisorb oxygen under similar experimental conditions employed for MoO_3/TiO_2 catalysts. The O_2 uptakes determined at 623 K for various MoO_3/TiO_2 (anatase) and MoO_3/TiO_2 (rutile) catalysts are given in Tables 1 and 2, respectively. A plot of oxygen uptake versus Mo loading (Fig. 3) suggests that at low Mo loadings the oxygen uptake approached a stoichiometry of one oxygen atom per molybdenum atom in TiO_2 (anatase) catalysts. Using this stoichiometry, Oyama et al. [13,14] defined the dispersion of molybdena as a fraction of total oxygen atoms (determined from oxygen chemisorption) to total Mo atoms in the sample. The changes in the dispersion of molybdena and the oxygen atom site density as a function of Mo loading

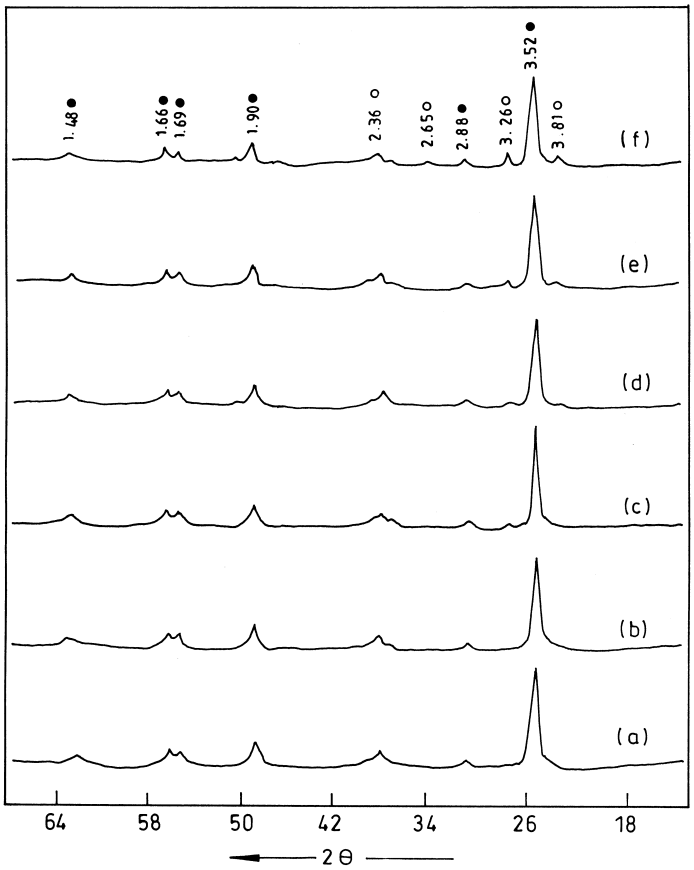

Fig. 1. X-ray diffractograms of MoO_3/TiO_2 (anatase) catalysts: (a) 2% Mo/TiO_2; (b) 4% Mo/TiO_2; (c) 6% Mo/TiO_2; (d) 8% Mo/TiO_2; (e) 10% Mo/TiO_2; (f) 12% Mo/TiO_2. (●) peaks due to TiO_2 (anatase); (○) peaks due to MoO_3.

are also reported in Tables 1 and 2. As can be seen from Tables 1 and 2, oxygen chemisorption capacities are found to increase with molybdenum loading upto 6 wt.% of Mo and level off at higher loadings. The levelling off is attributed to the formation of a monolayer of molybdenum oxide on titania. At high molybdenum loadings, no further increase of oxygen chemisorption was noticed. This might be due to the

Table 1
Results of oxygen uptake, dispersion, oxygen atom site density and surface area of various MoO_3/TiO_2 (anatase) catalysts

Catalyst composition (wt.% Mo)	Surface area[a] ($m^2 g^{-1}$)	Oxygen uptake[b] (μ mol g^{-1})	Oxygen atom site density (10^{18} m^{-2})	Dispersion[c] O/Mo
2	48	103.5	2.78	0.99
4	52	208.0	4.26	1.00
6	51	303.4	5.90	0.97
8	46	331.0	7.17	0.79
10	49	346.0	8.51	0.66
12	40	342.8	10.29	0.54

[a] BET surface area determined after oxygen chemisorption.
[b] $T_{(Reduction)} = T_{(Adsorption)} = 623$ K.
[c] Dispersion = Fraction of molybdenum atoms at the surface assuming $O_{ads}/Mo_{surf} = 1$.

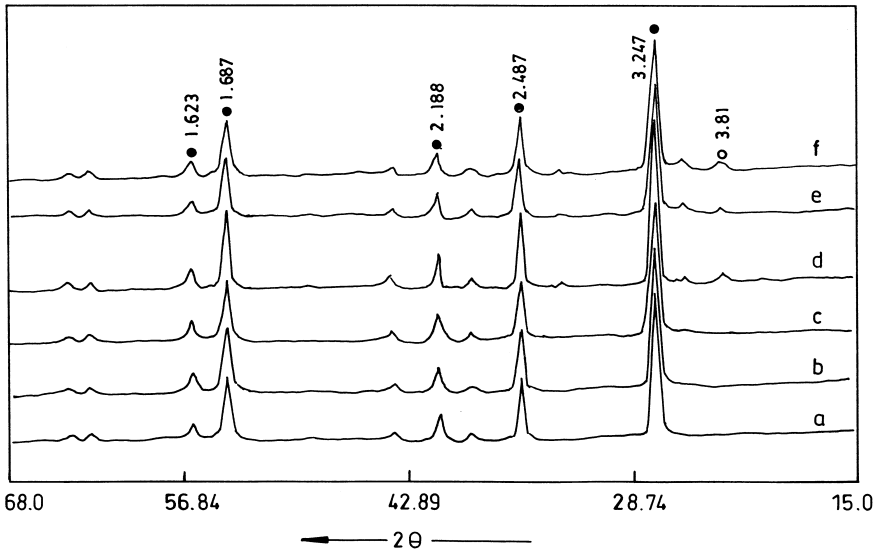

Fig. 2. X-ray diffractograms of MoO_3/TiO_2 (rutile) catalysts: (a) 2% Mo/TiO_2; (b) 4% Mo/TiO_2; (c) 6% Mo/TiO_2; (d) 8% Mo/TiO_2; (e) 10% Mo/TiO_2; (f) 12% Mo/TiO_2. (●) peaks due to TiO_2 (rutile); (○) peaks due to MoO_3.

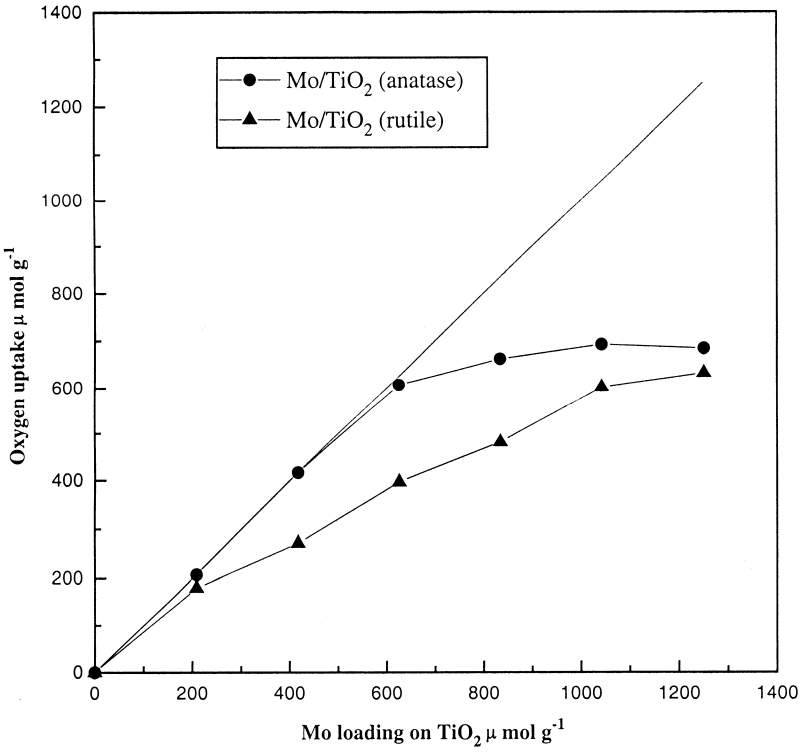

Fig. 3. Oxygen uptake plotted as a function of Mo loading on titania ($T_{adsorption} = T_{reduction} = 623\,K$).

Table 2
Results of oxygen uptake, dispersion, oxygen atom site density and surface area of various MoO_3/TiO_2 (rutile) catalysts

Catalyst composition (wt.% Mo)	Surface area[a] (m^2g^{-1})	Oxygen uptake[b] (μ mol g^{-1})	Oxygen atom site density (10^{18} m^{-2})	Dispersion[c] O/Mo
2	33	90.0	3.28	0.86
4	32	135.0	5.08	0.65
6	29	198.0	8.22	0.63
8	32	240.2	8.77	0.58
10	30	300.7	12.07	0.57
12	27	336.1	14.99	0.52

[a] BET surface area determined after oxygen chemisorption.
[b] $T_{(Reduction)} = T_{(Adsorption)} = 623$ K.
[c] Dispersion = Fraction of molybdenum atoms at the surface assuming $O_{ads}/Mo_{surf} = 1$.

presence of the crystalline molybdena phase, as seen in the XRD results, and which upon prereduction with hydrogen does not appreciably chemisorb oxygen. The oxygen atom site density values reported in Tables 1 and 2 suggest that the oxygen chemisorption in the plateau region is indeed titrating surface molybdenum atoms. The reduction behavior of supported molybdena catalysts prior to oxygen chemisorption is an interesting topic. Our results of oxygen chemisorption are in excellent agreement with those of Oyama et al. [14] on MoO_3/TiO_2 (anatase).

As mentioned earlier, in the present study the levelling off of oxygen chemisorption beyond the monolayer composition (above 6% Mo loading) might be due to the presence of larger crystallites of MoO_3, as evidenced from the XRD results (Figs. 1c–f and 2c–f). These larger crystallites of molybdenum oxide are preventing reduction of the catalyst with hydrogen gas; therefore, no appreciable change in oxygen uptake is observed for the catalysts beyond the monolayer composition. Based on the "patch" model of Hall [35], the nature of the oxygen chemisorption sites on Mo/Al_2O_3 catalysts has been discussed by Nag [15]. It has been envisaged that at lower Mo loadings small patches of molybdenum oxide, two layers thick and with Mo in an octahedral coordination, are formed on the support surface. Upon reduction, coordinatively unsaturated sites (CUS) of MoO_2 are generated by the removal of oxygen from the edge and corner sites of the patches [35]. These are the sites upon which oxygen chemisorption takes place. It has also been proposed that, as the Mo loading increases, the number of these patches increase with attendant increase in the number of CUS upto the monolayer level. Beyond the monolayer level, the patches grow three-dimensionally, thus decreasing the dispersion of molybdenum oxide. It is proposed that a similar mechanism operates in the $Mo\text{-}TiO_2$ system. The present results can be explained with the help of the above concepts. Thus, the initial increase and subsequent levelling off in the oxygen uptake capacity of the catalysts as a function of Mo loading is due to the generation of a new CUS up to monolayer level and a subsequent decrease in the edge and corner growth. A comparison of molybdena dispersion, measured with oxygen chemisorption method, suggests that MoO_3 supported on anatase TiO_2 show higher dispersion (Table 1) than the corresponding MoO_3/TiO_2 (rutile) samples (Table 2).

The TPR profile of unsupported MoO_3 has been presented in Fig. 4. The TPR profiles of pure MoO_3 show two major peaks at 1040 K, 1270 K and one minor reduction peak at 1070 K. For TPR analysis of unsupported MoO_3, the reduction conditions applied were similar to those of the supported MoO_3/TiO_2 catalysts. According to Thomas et al. [37] and Arnoldy et al. [41], the reduction of molybdena essentially can take place in two steps. The reducibility of MoO_3 is represented by the following steps:

$$MoO_3 \rightarrow MoO_2 \quad (1)$$

$$MoO_2 \rightarrow Mo \quad (2)$$

The sharp peak at 1040 K corresponds to the reduction of MoO_3 (first step) and the peak at 1270 K is associated with the reduction of the second step. A minor peak at the edge of the first major peak is observed at 1070 K, which corresponds to Mo_4O_{11} formed by

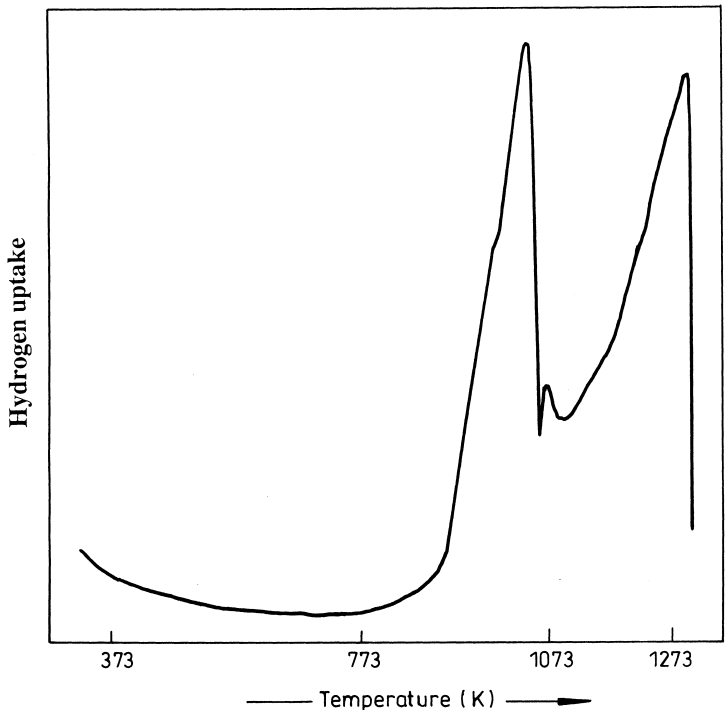

Fig. 4. Temperature programmed reduction (TPR) profile of unsupported MoO_3.

reduction of MoO_3. Thomas [38] also noticed this peak during TPR of MoO_3 and confirmed by in situ XRD

$$MoO_3 \rightarrow Mo_4O_{11} \quad (3)$$

The TPR profiles of MoO_3/TiO_2 (anatase) catalysts are presented in Fig. 5 and the TPR profiles of MoO_3/TiO_2 (rutile) catalysts are presented in Fig. 6. The reduction profiles of MoO_3/TiO_2 (rutile) catalysts show that the reduction occurs in two stages, and at higher loadings (i.e. above monolayer coverage), the reduction peak at a T_{max} of 873 K and the intensitiy of this peak are increasing with the increase of Mo loading. This uniform behaviour is not present in MoO_3/TiO_2 (anatase) catalysts. The TPR profiles of MoO_3/TiO_2 (anatase) reveals that, at low Mo loadings, additional small peaks can be seen before the major peaks. These are absent in catalysts containing higher Mo loadings. An examination of TPR profiles of unsupported MoO_3 and MoO_3 supported on TiO_2 indicates that the first reduction step for the molybdenum oxide species on titania occurs at much lower temperature than the first reduction step of bulk MoO_3. However, the difference in T_{max} is marginal for the second reduction in both bulk MoO_3 and supported catalysts. It has been reported that Mo^{6+} species can be present in both tetrahedral and octahedral coordination, and the particulate MoO_3 present at loadings above the monolayer value will have Mo^{6+} ions in the latter form [17]. On this basis, Bond and Tahir [17] also reported that the first two peaks at low MoO_3 content represent the reduction of Mo^{6+} in tetrahedral and octahedral coordination [39,40] to Mo^{4+}. The third peak in TPR of MoO_3/TiO_2 catalysts is due to the reduction of Mo^{4+} to Mo^0. The final peak must also be due to the same process, but must relate to the molybdenum, which was originally in octahedral coordination. It is likely that both the Mo^{4+} species are tetrahedral, so they are perhaps distinguished by being held on different crystal planes or in different states of aggregation. Bond and Tahir [17] have shown the models for structures of Mo^{6+} and Mo^{4+} ions on the surface of anatase.

The representative ^1H MAS NMR spectra of various MoO_3 catalysts supported on anatase and rutile

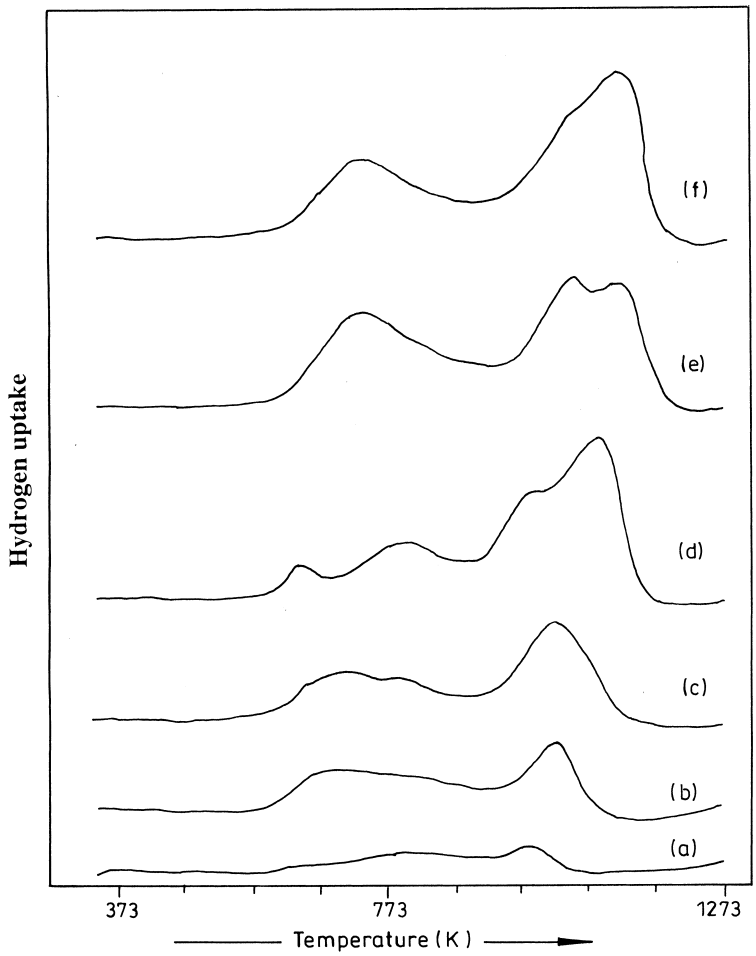

Fig. 5. Temperature programmed reduction (TPR) profiles of MoO_3/TiO_2 (anatase) catalysts: (a) 2% Mo/TiO_2; (b) 4% Mo/TiO_2; (c) 6% Mo/TiO_2; (d) 8% Mo/TiO_2; (e) 10% Mo/TiO_2; (f) 12% Mo/TiO_2.

modifications of TiO_2 are shown in Figs. 7 and 8, respectively. The dependence of the total signal intensity measured relative to the standard sample (SiO_2 evacuated at 573 K for 4 h contained 5×10^{19} OH groups) as a function of MoO_3 content for both anatase and rutile supported catalysts, is illustrated in Fig. 9.

Titanium oxide occurs in three crystallographic modifications viz., anatase, rutile and brookite. In all three forms, each Ti^{4+} ion is surrounded by six O^{2-} ions and each O^{2-} ion has three Ti^{4+} neighbors [42]. A clean (001) cleavage plane of anatase should have one O^{2-} ion missing in the coordination shell of each Ti^{4+} ion: the O^{2-} ions in the surface bridge two Ti^{4+} ions; the third coordinated Ti^{4+} is missing. The charges on Ti^{4+} and O^{2-} would nevertheless be balanced by the surrounding ions of opposite charge sign. The resulting formal charges would then be $-1/3$ and $+1/3$, respectively. According to Pauling's electrostatic valence rule [43], in a stable ionic structure the formation of hydroxyl groups on the surface of TiO_2 is favored. One would even expect two types of OH groups on the (001) face exhibiting somewhat different activity. Convincing chemical evidence for the presence of surface hydroxyl groups on titanium dioxide was presented by Lieflander and Stober [44]. According to previous work [42,45–49], the anatase surface consists predominantly of the most dense (001) plane, with admixture of (010) and (100) plane

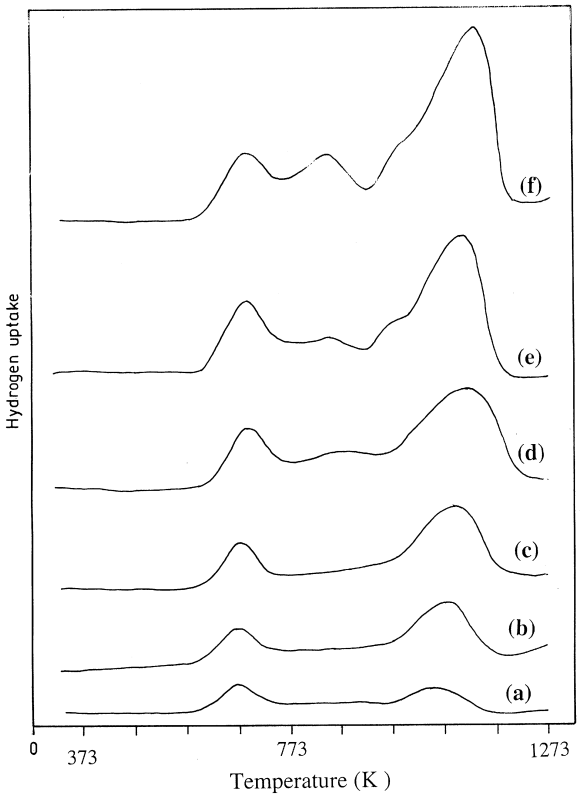

Fig. 6. Temperature programmed reduction (TPR) profiles of MoO_3/TiO_2 (rutile) catalysts: (a) 2% Mo/TiO_2; (b) 4% Mo/TiO_2; (c) 6% Mo/TiO_2; (d) 8% Mo/TiO_2; (e) 10% Mo/TiO_2; (f) 12% Mo/TiO_2.

having about the same structures. Ti atoms in these planes are pentacoordinated with respect to oxygen. There are two types of oxygen atoms on each (001), (010) and (100) plane of TiO_2 surface. Oxygen atoms of the first type are coordinated to Ti atoms and have a formal charge $-2/3$, assuming all the bonds in TiO_2 are purely ionic. They are located 0.41 Å above the (001) plane. The oxygen atoms of second type located 0.41 Å below (001) plane, are three coordinated to Ti atoms. For (010) and (100) planes, all oxygen atoms are located in the plane. Yates [49] found the existence of two types of OH groups on the anatase surface and this was confirmed by the infra-red studies (two stretching infrared absorption bands at 3715 and 3675 cm^{-1}). These results were confirmed by Smith [51]. The band at 3675 cm^{-1} corresponds to the adjacent OH groups interacting via weak hydrogen

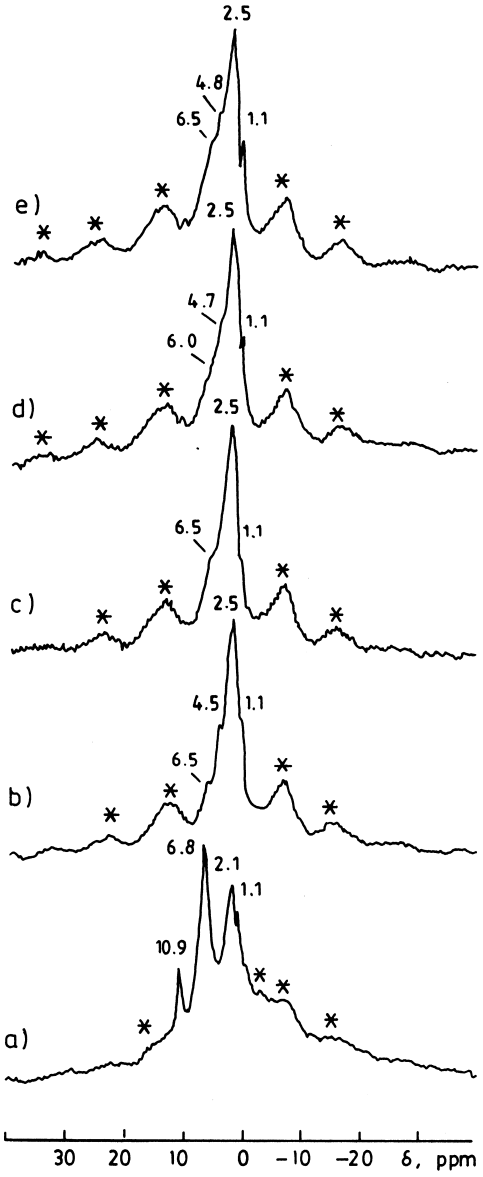

Fig. 7. ^1H NMR MAS spectra of TiO_2 (anatase) and MoO_3/TiO_2 (anatase) samples at various 'Mo' levels (ref: [31]): (a) TiO_2 (anatase); (b) 2% Mo; (c) 4% Mo; (d) 8% Mo; (e) 10% Mo.

bonds, while the band at 3715 cm^{-1} can be attributed to OH groups attached to Ti atoms. Primet et al. [46] have studied the adsorption of various probe molecules and found the existence of different hydroxyl groups on two modifications of titania using infra-red spectroscopy; possible structures of surface

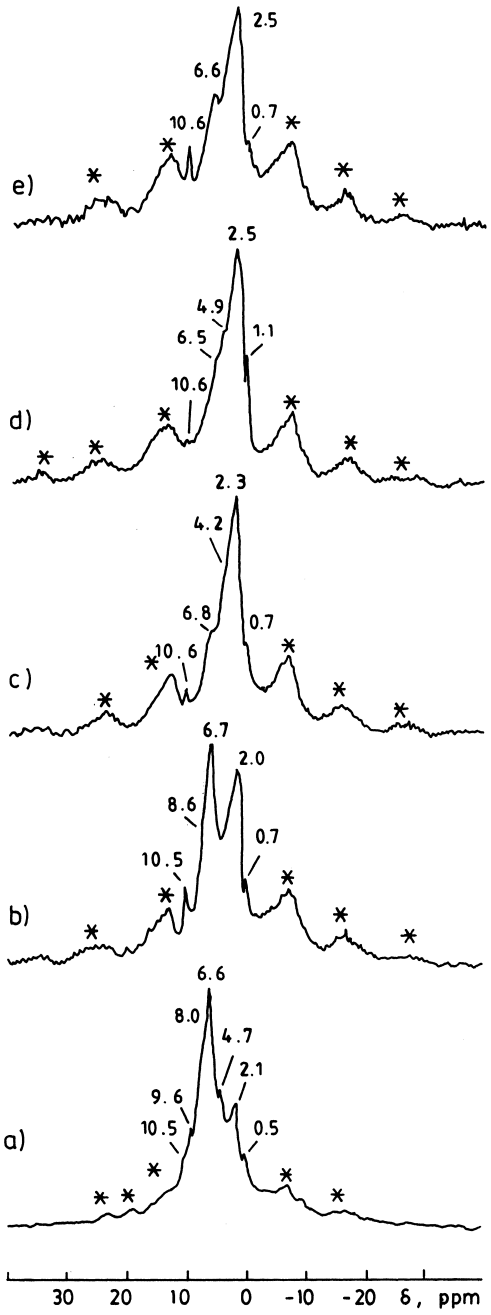

Fig. 8. ^{1}H NMR MAS spectra of TiO_2 (rutile) and MoO_3/TiO_2 (rutile) samples at various 'Mo' levels (ref: [31]): (a) TiO_2 (rutile); (b) 2% Mo; (c) 4% Mo; (d) 8% Mo; (e) 10% Mo.

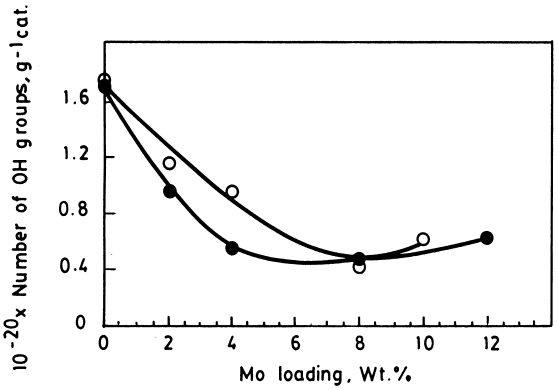

Fig. 9. The concentration of the surface OH groups as function of Mo content on various MoO_3/TiO_2 catalysts (ref: [31]): (●) Mo/anatase; (○) Mo/rutile.

hydroxyl groups on titania have been discussed [47]. Tanaka and White [50] reported that similar types of OH groups are also characteristic for rutile TiO_2. The observation of two main peaks in the ^{1}H MAS NMR spectra of the molybdenum oxide catalysts, supported on anatase and rutile samples of the present study, are in agreement with this model. The down field peak at $\delta \approx 6.5$ ppm can be attributed to 'acidic' OH groups coordinated to two Ti atoms, while the signal with $\delta \approx 2.1$–2.5 ppm is more likely to belong to 'basic' OH groups coordinated to one Ti atom. The low field peak most probably can be ascribed to the more acidic OH groups localized on bridging oxygen atoms and forming weak hydrogen bonds with adjacent oxygen atoms [32]. The high field peak was ascribed to the more basic OH groups, where hydrogen atoms are bound with terminal oxygen atoms. The unidentified sharp line at $\delta \approx 10.9$ ppm most probably belongs to some OH groups associated with impurities present in the samples under study [32].

Height and Boston [52] pointed out that, at high pH regions (> 6), MoO_4^{2-} ions are generally present in solution, but at acidic pH regions ($1 < pH < 6$) MoO_4^{2-} gives $Mo_7O_{24}^{6-}$ and $Mo_8O_{26}^{4-}$ ions. The hydroxyl groups of the titania surface in solution tend to be either positively or negatively charged below or above the IEP of titania (anatase: pH 6.2, rutile: pH 4.8 to 5.6) [53,54]. The results presented in Figs. 7 and 8 unambiguously show the selective interaction of Mo atoms with the 'acidic' Ti-OH groups while the 'basic' OH groups remain unperturbed when MoO_3 is suppor-

ted on the TiO_2 surface. The OH groups of anatase and rutile show a basic character towards compounds, like CO_2, with a pK_{ab} value lower than 6.5 [46]. The impurity OH group also decreases in the sample with supported MoO_3. The decrease of the NMR signal intensity proceeds rapidly at the lowest concentration (2% Mo w/w on TiO_2) studied; thereafter the decrease in intensity becomes much less pronounced (Fig. 9). This is the case for both anatase and rutile-supported molybdena catalyst samples. It should be noted that the largest Mo concentration (12% Mo w/w on TiO_2) is larger than the formal 'monolayer' amount of MoO_3. This observation of MoO_3 on the TiO_2 surface is in agreement with the 'patchy-monolayer' model of Mo/Al_2O_3 catalysts discussed elsewhere [15].

As can be seen from Fig. 9, a comparison of the quantity of reacted OH groups with the quantity of adsorbed Mo atoms reveals that, at the lowest content of molybdenum (2% Mo w/w on TiO_2), each Mo atom reacts with approximately one OH group. However, at higher Mo contents, several Mo atoms are required for the interaction with one OH group. Therefore, most probably at the low Mo (2%) concentration in the catalyst, monomeric isolated Mo species are formed, while at the larger concentration of Mo in the catalysts, most probably the clusters containing several Mo atoms are created on the TiO_2 surface. Mastikhin and Nosov [32] reported a ^1H MAS NMR study of the TiO_2 prepared from various methods and found two types of hydroxyl groups present on titania. Thus, ^1H MAS NMR spectra of MoO_3 catalysts supported on anatase and rutile polymorphs reveal the presence of two types of OH groups on the surface: one ascribed to OH groups of acidic nature and other to basic OH groups.

It is interesting to study the nature of the interaction of molybdenum oxide with supported oxides. Many

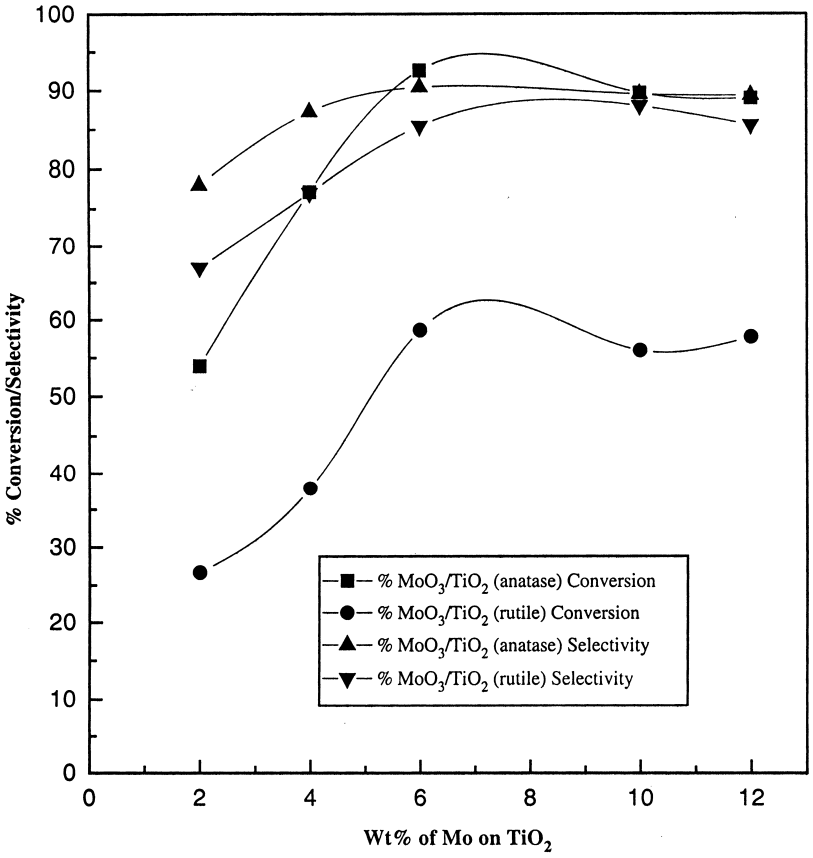

Fig. 10. Ammoxidation of 3-picoline over MoO_3/TiO_2 (anatase) and MoO_3/TiO_2 (rutile) catalysts (reaction temperature 683 K).

authors [11,13,14,24–27] reported the nature of the interaction of molybdenum oxide with alumina, silica and titania. Desikan et al. [13,14] reported from IR and Raman spectroscopy studies that molybdenum oxide interacts more strongly with titania than other supported systems. Kim et al. [24–27] investigated molecular structures of the molybdenum oxides over different oxide supports using Raman spectroscopy under ambient conditions. They suggested that surface structures of molybdenum oxide species for calcined MoO_3/supports catalysts exposed to ambient conditions are dependent on the net surface pH at PZC. The results of dispersion of molybdenum oxide and its reducibility by TPR of the present investigation suggest that molybdenum oxide interacts more strongly with TiO_2 (anatase) than when it is supported on TiO_2 (rutile).

The catalytic properties were evaluated for ammoxidation of 3-picoline to nicotinonitrile over molybdena supported on anatase and rutile titania at 683 K; the results are presented in Fig. 10. As can be seen from Fig. 10, the conversion of 3-picoline and selectivity towards nicotinonitrile formation were found to increase with the increase of Mo loading on both the morphologies of titania. The conversion of 3-picoline did not appreciably change beyond 6 wt.% of Mo on TiO_2 (anatase) and TiO_2 (rutile). However, the selectivity of the nicotinonitrile formation was found to be independent of Mo content in all the catalysts. Pure titania was found to be inactive during the ammoxidation of 3-picoline under the experimental conditions.

To find the relation between the ammoxidation activity of 3-picoline and the dispersion of molybdena on TiO_2 (anatase) and TiO_2 (rutile), a plot of TOF versus the number of surface Mo content is shown in Figs. 11 and 12, respectively, where TOF is equal to the rate of 3-picoline molecules converted per second per surface Mo. As can be seen from Fig. 11, an initial

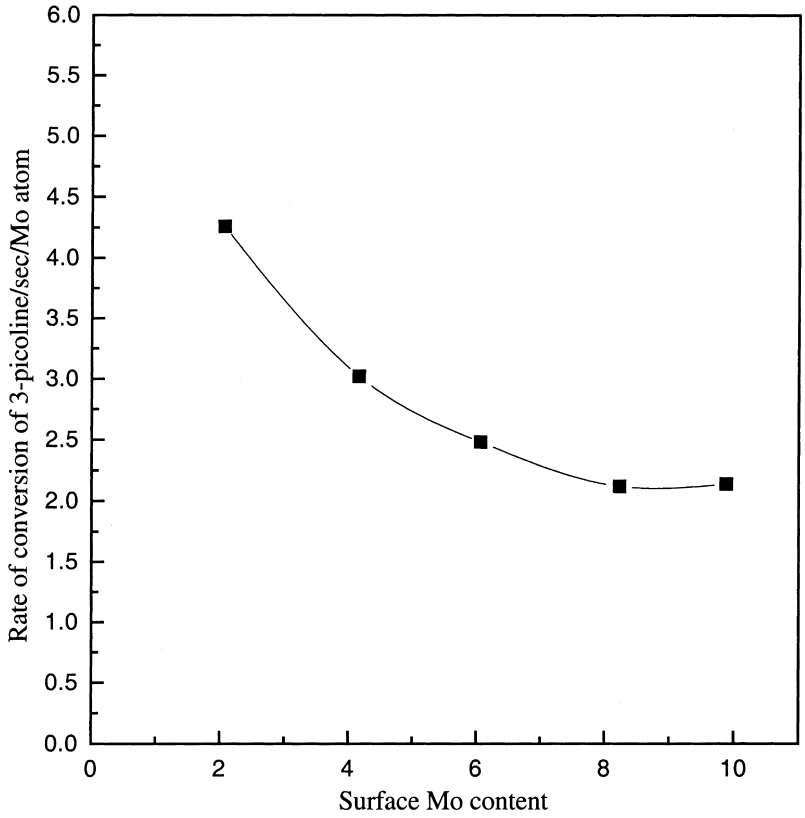

Fig. 11. Relationship between the number of surface Mo moles and the rate of 3-picoline conversion on MoO_3/TiO_2 (anatase) catalysts.

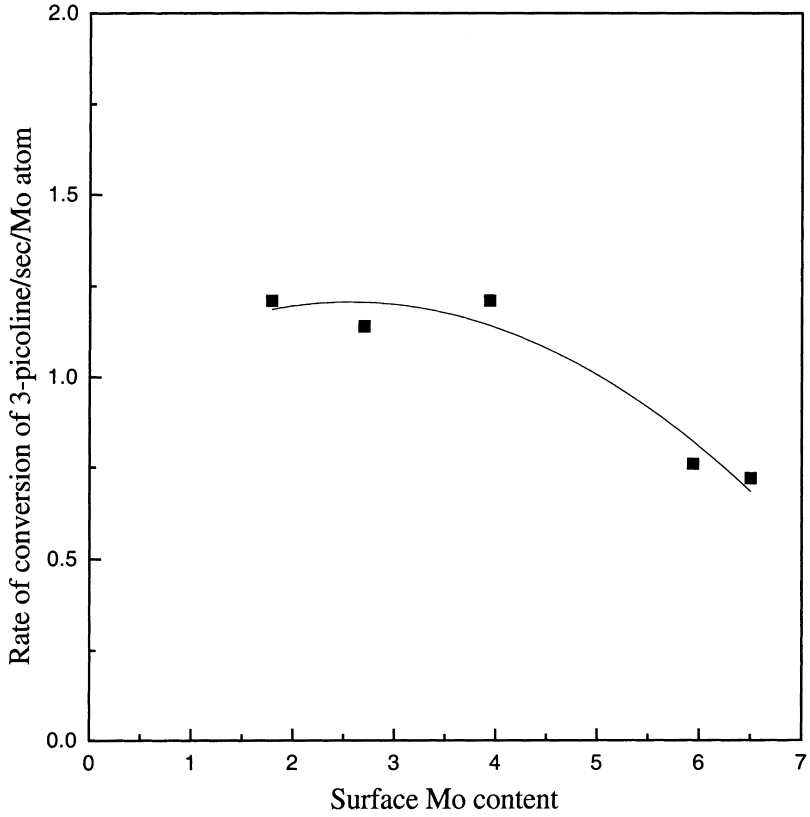

Fig. 12. Relationship between the number of surface Mo moles and the rate of 3-picoline conversion on MoO_3/TiO_2 (rutile) catalysts.

decrease in TOF and constant value beyond 6 wt.% Mo are observed. On TiO_2 (rutile) (Fig. 12), a constant TOF value is observed at low molybdena loading (upto 6 wt.%), beyond which a sharp fall is observed. The constancy in TOF value beyond 6 wt.% Mo on TiO_2 (anatase) indicates the attainment of bulk nature of MoO_3 and below 6 wt.% Mo loading on TiO_2 (anatase) the continuous decrease in TOF indicates that the persite activity is decreasing drastically even though the number of surface Mo sites are increasing. On Mo supported on TiO_2 (rutile) upto 6 wt.% loading, the persite activity is constant with the increase in surface Mo sites. The decrease in TOF beyond 6 wt.% loading indicates the formation of bigger MoO_3 particles, but not enough to attain the bulk nature on Mo supported on TiO_2 (rutile). It can be concluded from Figs. 11 and 12 that the ammoxidation of 3-picoline has higher acitivity for MoO_3/TiO_2 (anatase) compared to those observed with MoO_3 supported on TiO_2 (rutile). Thus, oxygen chemisorption can be used to find the effect of support on the ammoxidation activity. The absence of direct correlation between TOF and surface MoO_3 molecules may be due to the fact that, in addition to oxygen adsorption, ammonia adsorption may also be responsible for this reaction.

As reported elsewhere in connection with molybdenum oxide catalysts supported on alumina [15] and on zirconia [55], oxygen is chemisorbed at low temperatures selectively on CUS, generated upon reduction, having a particular coordination environment. These sites are located on a highly dispersed molybdenum phase, which is formed only at low molybdenum loadings, and, remain as a “patchy monolayer” on the support surface. At higher molybdena loadings, a second phase is formed in addition to the already existing monolayer, and this post monolayer phase does not appreciably chemisorb oxygen (Fig. 3). In the perspective of the above background, this correlation

indicates that the catalytic functionality of the dispersed molybdena phase supported on titania is responsible for the ammoxidation of 3-picoline to nicotinonitrile that is located on a patchy-monolayer phase, which can be titrated by the oxygen chemisorption method.

4. Conclusions

Oxygen chemisorption measured at 623 K on the catalysts reduced at the same temperature provides a better measure of dispersion of molybdenum oxide supported on titania. MoO_3 disperses better on anatase TiO_2 than when it is supported on rutile TiO_2. ^1H MAS NMR spectra of MoO_3 catalysts supported on anatase and rutile polymorphs reveal the presence of two types of OH groups on the surface: one ascribed to OH groups of acidic nature and other to basic OH groups. TPR profiles suggest that the reduction of MoO_3 occurs in two stages. The catalytic activity during 3-picoline ammoxidation is directly related to dispersion of molybdenum.

Acknowledgements

K.V.R. Chary thanks EMR Division of Council of Scientific and Industrial Research (CSIR), New Delhi, for financial support under the CSIR young scientist award scheme. T. Bhaskar thanks CSIR, New Delhi, for the award of Research Associateship; K.R. Reddy thanks CSIR, New Delhi, for the award of Junior Research Fellowship and K. Sri Lakshmi and K.K. Seela thank Director, IICT, for Project Trainee positions. We are also grateful to Ti-Oxide UK Ltd. for providing anatase and rutile TiO_2.

References

[1] F.E. Massooth, Adv. Catal. 27 (1978) 265.
[2] H. Knozinger, in: M. Phillips, M. Ternan (Eds.), Proceedings of the 9th International Congress on Catalysis, Calgary, 1988, Vol. 5, The Chemical Institute of Canada, Ottawa, 1989, p. 20.
[3] B.M. Reddy, K.V.R. Chary, V.S. Subrahmanyam, N.K. Nag, J. Chem. Soc., Faraday Trans. I 81 (1985) 1655.
[4] K.Y.S. Ng, E. Gulari, J. Catal. 95 (1985) 33.
[5] Y.C. Liu, G.L. Griffin, S.S. Chan, I.E. Wachs, J. Catal. 94 (1985) 94, 108.
[6] Y. Masuoka, M. Niwa, Y. Murakami, J. Phys. Chem. 94 (1990) 1477.
[7] W. Zhang, A. Desikan, S.T. Oyama, J. Phys. Chem. 99 (1995) 14468.
[8] K.V.R. Chary, V.V. Kumar, P. Kanta Rao, Langmuir 6 (1990) 1549.
[9] A.N. Desikan, W. Zhang, S.T. Oyama, J. Catal. 157 (1995) 740.
[10] H. Miyata, T. Mukai, T. Ono, Y. Kubokawa, J. Chem. Soc., Faraday Trans. I 84 (1988) 4137.
[11] N.K. Nag, J. Phys. Chem. 91 (1987) 2324.
[12] B.R. Quincy, M. Houalla, A. Proctor, D.M. Hercules, J. Phys. Chem. 94 (1990) 1520.
[13] A.N. Desikan, L. Huang, S.T. Oyama, J. Phys. Chem. 95 (1991) 10050.
[14] A.N. Desikan, L. Huang, S.T. Oyama, J. Chem. Soc., Faraday Trans. 88 (1992) 3357.
[15] N.K. Nag, J. Catal. 92 (1985) 432.
[16] T. Machej, B. Doumain, B. Yasse, B. Delmon, J. Chem. Soc., Faraday Trans. I 84 (1988) 3905.
[17] G.C. Bond, S.F. Tahir, Appl. Catal. 105 (1993) 281.
[18] K.Y.S. Ng, E. Gulari, J. Catal. 92 (1985) 340.
[19] D.M. Arco, J.M. Holgado, C. Martin, V. Rives, J. Catal. 99 (1986) 19.
[20] T. Machej, J. Haber, M.A. Turek, I.E. Wachs, Appl. Catal. 70 (1991) 115.
[21] Y. Okamoto, A. Maezawa, T. Imanaka, J. Catal. 120 (1989) 29.
[22] A.J. Van Hengstum, J.G. Van Ommen, H. Bosch, P.J. Gellings, Appl. Catal. 5 (1983) 207.
[23] R.B. Quincy, M. Houlla, D.M. Hercules, J. Catal. 106 (1987) 85.
[24] D.S. Kim, Y. Kurusu, I.E. Wachs, F.D. Hardcastle, K. Segawa, J. Catal. 120 (1989) 325.
[25] K. Segawa, D.S. Kim, Y. Kurusu, I.E. Wachs, in: M.J. Phillips, M. Ternan (Eds.), Proccedings of the 9th International Congress on Catalysis, Calgary, 1988, Chem. Institute of Canada, Ottawa, 1988, p. 1960.
[26] D.S. Kim, K. Segawa, T. Soeya, I.E. Wachs, J. Catal. 136 (1992) 539.
[27] D.S. Kim, I.E. Wachs, K. Segawa, J. Catal. 146 (1994) 268.
[28] S.J. Tauster, S.C. Fung, R.L. Garten, J. Am. Chem. Soc. 100 (1978) 170.
[29] V.M. Mastikhin, I.L. Mudrakovsky, A.V. Nosov, Progr. NMR Spectrosc. 23 (1991) 259.
[30] M.A. Enriquez, M.C. Doremeux, J.J. Fraissard, J. Solid State Chem. 40 (1981) 233.
[31] K.V.R. Chary, V.V. Kumar, P. Kanta Rao, A.V. Nosov, V.M. Mastikhin, J. Mol. Catal. A. Chemical 96 (1995) L5.
[32] V.M. Mastikhin, A.V. Nosov, React. Kinet. Catal. Lett. 46 (1992) 123.
[33] K.V.R. Chary, G. Kishan, J. Phys. Chem. 99 (1995) 14424.
[34] B.S. Parekh, S.W. Weller, J. Catal. 40 (1987) 100.
[35] W.K. Hall, in: H.F.Barry, P.C.H. Mitchel (Eds.), Proceedings of the Fourth International Conference on the Chemistry and Uses of Molybdenum, Climax Molybdenum Co., Ann Arbor, MI, 1982, p. 224.

[36] K.V.R. Chary, T. Bhaskar, G. Kishan, V. Vijaya Kumar, J. Phys. Chem. 102 (1998) 3936.
[37] R. Thomas, V.H.J. de Beer, J.A. Moulijn, Bull. Chim. Belg. 90 (12) (1981).
[38] R. Thomas, Ph.D. thesis, University of Amsterdam, 1981.
[39] J. Bernholc, J.A. Horsley, L.L. Murrell, L.G. Sherman, S. Soled, J. Phys. chem. 81 (1987) 1526.
[40] M. Cornac, A. Janin, J.C. Lavelley, Polyhedron 5 (1986) 183.
[41] P. Arnoldy, J.C.M. de Jonge, J.A. Mouljin, J. Phys. Chem. 89 (1985) 4517.
[42] H.P. Boehm, Adv. Catal. 16 (1966) 179.
[43] L. Pauling, The Nature of the Chemical Bond, 3rd Edition, Cornell Univ. Press, New York, 1960, p. 548.
[44] M. Lieflander, W. Stobber, Z. Naturforsch. 15b (1960) 411.
[45] H. Knozinger, Adv. Catal. 25 (1982) 184.
[46] M. Primet, P. Pichat, M.V. Mathieu, J. Phys. Chem. 75 (1971) 1221.
[47] M. Primet, P. Pichat, M.V. Mathieu, J. Phys. Chem. 75 (1971) 1216.
[48] M. Primet, P. Pichat, M.V. Mathieu, CR Acad. Sci. Ser. B 267 (1986) 799.
[49] D.J.C. Yates, J. Phys. Chem. 65 (1961) 746.
[50] K. Tanaka, J.M. White, J. Phys. Chem. 86 (1982) 4708.
[51] I.T. Smith, Nature 67 (1964) 201.
[52] G.P. Height, D.R. Boston, in: P.C.H. Mitchell (Ed.), Proceedings of the 1st International Climax. Conference on the Chemistry and Uses of Molybdenum, London, 1973, p. 48.
[53] G.A. Parks, Chem. Rev. 65 (1965) 177.
[54] G.D. Parfitt, Pure. Appl. Chem. 48 (1976) 415.
[55] B.M. Reddy, K.V.R. Chary, B.R. Rao, C.S. Sunandana, V.S. Subrahmanyam, N.K. Nag, Polyhedron 5 (1996) 191.